The EMBO Journal (2010) 29, 1748–1761 | © 2010 European Molecular Biology Organization | All Rights Reserved 0261-4189/10
www.embojournal.org

THE EMBO JOURNAL

The Cullin 3 substrate adaptor KLHL20 mediates DAPK ubiquitination to control interferon responses

Yu-Ru Lee[1,2], Wei-Chien Yuan[1,3], Hsuan-Chung Ho[2], Chun-Hau Chen[1,2], Hsiu-Ming Shih[4] and Ruey-Hwa Chen[1,2,3,*]

[1]Institute of Biological Chemistry, Academia Sinica, Taipei, Taiwan, [2]Institute of Molecular Medicine, College of Medicine, National Taiwan University, Taipei, Taiwan, [3]Institute of Biochemical Sciences, College of Life Science, National Taiwan University, Taipei, Taiwan and [4]Institute of Biomedical Sciences, Academia Sinica, Taipei, Taiwan

Death-associated protein kinase (DAPK) was identified as a mediator of interferon (IFN)-induced cell death. How IFN controls DAPK activation remains largely unknown. Here, we identify the BTB–Kelch protein KLHL20 as a negative regulator of DAPK. KLHL20 binds DAPK and Cullin 3 (Cul3) *via* its Kelch-repeat domain and BTB domain, respectively. The KLHL20–Cul3–ROC1 E3 ligase complex promotes DAPK polyubiquitination, thereby inducing the proteasomal degradation of DAPK. Accordingly, depletion of KLHL20 diminishes DAPK ubiquitination and degradation. The KLHL20-mediated DAPK ubiquitination is suppressed in cells receiving IFN-α or IFN-γ, which induces an enrichment/sequestration of KLHL20 in the PML nuclear bodies, thereby separating KLHL20 from DAPK. Consequently, IFN triggers the stabilization of DAPK. This mechanism of DAPK stabilization is crucial for determining IFN responsiveness of tumor cells and contributes to IFN-induced autophagy. This study identifies KLHL20–Cul3–ROC1 as an E3 ligase for DAPK ubiquitination and reveals a regulatory mechanism of DAPK, through blocking its accessibility to this E3 ligase, in IFN-induced apoptotic and autophagic death. Our findings may be relevant to the problem of IFN resistance in cancer therapy.

The EMBO Journal (2010) **29,** 1748–1761. doi:10.1038/emboj.2010.62; Published online 13 April 2010
Subject Categories: signal transduction; differentiation & death
Keywords: BTB domain; Cullin 3; DAPK; interferon; PML nuclear bodies

Introduction

Interferons (IFNs) possess antitumor activities mainly through their inhibition of growth and induction of tumor cell apoptosis and have been used to treat a variety of cancers, including several hematological neoplasms (Gutterman, 1994; Strander and Einhorn, 1996). Despite their wide use, the mechanisms underlying their antitumor activities have not been fully understood, and therefore the factors responsible for IFN resistance remain largely elusive.

Death-associated protein kinase (DAPK) is a calmodulin-regulated serine/threonine kinase. Several lines of evidence suggest that DAPK is a tumor suppressor. First, in a wide range of human cancers, DAPK promoter has been found to be silenced by methylation (Bialik and Kimchi, 2004). In virtually in all sporadic cases of chronic lymphocytic leukemia, for instance, DAPK has been observed to be silenced epigenetically (Raval *et al*, 2007). DAPK downregulation in human tumors can also be caused by genetic (Raval *et al*, 2007) and posttranslational mechanisms (Wang *et al*, 2007). Second, in several types of human cancers, loss of DAPK expression correlates strongly with the recurrence and metastatic progression (Bialik and Kimchi, 2004). Third, the antitumorigenic effect of DAPK has been directly evident in a mouse model in which DAPK expression has a causative function in suppressing the ability of Lewis lung carcinoma to form metastases in mice (Inbal *et al*, 1997). Finally, experiments using various cell culture systems have shown that DAPK has a critical function in promoting cell death (Deiss *et al*, 1995; Cohen *et al*, 1999; Raveh *et al*, 2001; Jang *et al*, 2002; Pelled *et al*, 2002; Wang *et al*, 2002; Llambi *et al*, 2005; Eisenberg-Lerner and Kimchi, 2007; Gozuacik *et al*, 2008; Castets *et al*, 2009) as well as in inhibiting cell migration and tumor invasion (Kuo *et al*, 2006), which likely contribute to the suppression of human malignancy.

DAPK was originally identified by a functional screen for genes whose inactivation protects cells from IFN-γ-induced cell death (Deiss *et al*, 1995). Subsequent studies have shown that DAPK acts as a positive mediator or regulator of apoptosis in response to a wide variety of stimuli, including TNF-α, Fas (Cohen *et al*, 1999), TGF-β (Jang *et al*, 2002), ceramide (Pelled *et al*, 2002), oncogene activation (Raveh *et al*, 2001), unliganded netrin receptor (Llambi *et al*, 2005; Castets *et al*, 2009), matrix detachment (Wang *et al*, 2002), and ER stress (Gozuacik *et al*, 2008). In addition to participating in the type-I programmed cell death, DAPK has been shown to mediate autophagic type-II cell death and caspase-independent necrotic cell death under certain cellular settings (Inbal *et al*, 2002; Eisenberg-Lerner and Kimchi, 2007). Consistent with its involvement in multiple modes of cell death, DAPK triggers the activation of a number of death-promoting pathways, depending on cell types and contexts. For instance, DAPK induces a p53-dependent apoptotic checkpoint in response to oncogenic activation (Raveh *et al*, 2001) and activates PKD/JNK pathway under oxidative stress (Eisenberg-Lerner and Kimchi, 2007). The integrin-inactivating activity of DAPK contributes to its induction of anoikis (Wang *et al*, 2002), whereas its phosphorylation of myosin regulatory light chain (Bialik *et al*, 2004) and interaction with MAP1B (Harrison *et al*, 2008) are linked to

*Corresponding author. Institute of Biological Chemistry, Academia Sinica, 128 Academia Road Sec. II, Taipei 115, Taiwan.
Tel.: +886 2 2785 5696/Ext. 6020; Fax: +886 2 2788 9759;
E-mail: rhchen@gate.sinica.edu.tw

Received: 29 November 2009; accepted: 18 March 2010; published online: 13 April 2010

apoptotic membrane blebbing. Finally, phosphorylation of beclin 1 is a key event mediating DAPK-induced autophagy (Zalckvar *et al*, 2009). Although DAPK has a broad array of functions in promoting cell death induced by various stimuli, how DAPK itself is regulated or modified during these death processes remains poorly understood.

The ubiquitin-proteasome system has been found to be central to the control of protein turnover, thereby regulating numerous biological processes (Hershko and Ciechanover, 1998). In this system, proteins are tagged with ubiquitin moiety through a cascade of enzymatic reactions involving E1 activating enzyme, E2 conjugation enzyme, and E3 ubiquitin ligase. Cullin-based multi-protein complexes are the largest family of E3 ligase, in which Cullin serves as a scaffold for linking two functional modules: the catalytic RING finger protein ROC1 for recruiting E2, and the substrate-binding molecule for bringing substrate within the proximity to the catalytic module (Jackson and Eldridge, 2002; Cardozo and Pagano, 2004; Willems *et al*, 2004; Petroski and Deshaies, 2005; Bosu and Kipreos, 2008). The SCF complex, which consists of Skp1-Cul1-F-box-ROC1, is the best characterized Cullin family E3 ligase (Deshaies, 1999). More recently, the molecular architecture of Cul3-based E3 ligase complex has been determined (Furukawa *et al*, 2003; Geyer *et al*, 2003; Krek, 2003; Pintard *et al*, 2003, 2004; Xu *et al*, 2003; Cardozo and Pagano, 2004; Willems *et al*, 2004). In this complex, the Bric-a-brac/Tramtrack/Broad (BTB) complex domain-containing protein functions as the substrate adaptor to bridge Cul3 and substrate, which is analogous to the Skp1-F-box heterodimer in the SCF complex. The human genome encodes >180 BTB proteins (Stogios *et al*, 2005), suggesting that there is a large number of Cul3-BTB substrates. However, only a few substrates have been identified to date, and the physiological functions of most BTB proteins have not been studied. One of the well-characterized BTB proteins is Keap1, which regulates the stability of transcription factor Nrf2, thereby controlling the expression of a number of antioxidant genes (Cullinan *et al*, 2004; Kobayashi *et al*, 2004; Zhang *et al*, 2004; Furukawa and Xiong, 2005). Unlike the SCF substrates that often require phosphorylation for binding to F-box proteins, posttranslational modification is dispensable for the binding of Nrf2 to Keap1 (Lo *et al*, 2006; Padmanabhan *et al*, 2006, 2008; Tong *et al*, 2006) and therefore Nrf2 is constitutively targeted for Keap1-dependent degradation under basal conditions. In response to oxidative stress, Keap1 activity is impaired by oxidative modifications on specific cysteine residues, leading to Nrf2 stabilization (Zhang and Hannink, 2003; Wakabayashi *et al*, 2004).

In this study, we identify the BTB protein KLHL20 that functions as a substrate adaptor bringing DAPK to Cul3, thereby promoting DAPK ubiquitination and proteasomal degradation. In IFN-treated cells, the enrichment and sequestration of KLHL20 in PML nuclear bodies (PML-NBs) disrupts KLHL20–DAPK complex, thus impairing DAPK ubiquitination by KLHL20. This IFN-induced stabilization of DAPK contributes in part to the cell death effect of IFN and has a function in determining the tumor cell responsiveness to IFN. Thus, our study not only identifies the KLHL20–Cul3–ROC1 complex as an E3 ligase for DAPK ubiquitination, but also unravels the regulatory mechanism of DAPK in IFN-induced cell death.

Results

KLHL20 forms a complex with Cul3 and DAPK

In a search for potential interaction partners of DAPK, we performed a yeast two-hybrid screening of a human placenta cDNA library using the death domain (DD) of DAPK as bait. Several of the cDNA fragments we identified were encoded for the C-terminal region of a BTB/Kelch protein KLHL20, also known as KLEIP (Hara *et al*, 2004). The specificity of interaction between DAPK DD and KLHL20 (174–609) was verified by one-on-one transformation assay (Figure 1A). To determine whether the two proteins would interact in mammalian cells, we transfected 293T cells with epitope-tagged DAPK and KLHL20. Reciprocal immunoprecipitation analysis showed that DAPK bound specifically to KLHL20 (Supplementary Figure S1). To investigate whether these two proteins would interact endogenously, we generated an antiserum that could specifically recognize endogenous KLHL20 (Supplementary Figure S2). Using this antiserum, we found an association between endogenous KLHL20 and endogenous DAPK in HeLa cells (Figure 1B). The interaction between the two did not require DAPK catalytic activity, as the kinase-defective (K42A) and kinase-active (ΔCaM) mutants bound KLHL20 as effectively as the wild-type DAPK (Supplementary Figure S3). However, deletion of DD significantly diminished the ability of DAPK to bind endogenous KLHL20 (Figure 1C). To determine the region of KLHL20 responsible for binding DAPK, we generated KLHL20ΔB and KLHL20ΔK, which lack BTB domain and Kelch-repeat domain, respectively. Although KLHL20ΔB bound DAPK, KLHL20ΔK did not (Figure 1D). Together, these findings indicate that KLHL20 is a DAPK-interacting protein and the DD of DAPK and Kelch-repeat domain of KLHL20 are responsible for the interaction between the two proteins.

Recent studies have revealed that a number of BTB proteins function as substrate adaptors for Cul3-based E3 ligase (Furukawa *et al*, 2003; Geyer *et al*, 2003; Krek, 2003; Pintard *et al*, 2003, 2004; Xu *et al*, 2003; Cardozo and Pagano, 2004; Willems *et al*, 2004). Likewise, KLHL20 interacted with Cul3. Furthermore, deletion of its BTB domain rather than the Kelch-repeat domain, abrogated Cul3-binding ability of KLHL20, thus showing the critical function of BTB domain in Cul3 interaction (Figure 1E). The involvement of different domains of KLHL20 in the bindings of Cul3 and DAPK suggests a possible Cul3–KLHL20–DAPK tripartite complex. Indeed, when cells cotransfected with DAPK, KLHL20, and Cul3 were subjected to immunoprecipitation, both KLHL20 and Cul3 were coprecipitated with DAPK (Figure 1F). Furthermore, interaction of endogenous Cul3 with endogenous DAPK was detected in HeLa cells (Figure 1G). To confirm that this interaction was mediated by KLHL20, endogenous KLHL20 was downregulated by two different siRNAs. This depletion of KLHL20 significantly impaired the interaction of Cul3 with DAPK. Together, our data show the formation of Cul3–KLHL20–DAPK tripartite complex, in which KLHL20 binds Cul3 and DAPK through its BTB domain and Kelch-repeat domain, respectively.

KLHL20-based Cul3 complex promotes DAPK ubiquitination in vitro and in vivo

To investigate whether the KLHL20–Cul3 complex could promote the ubiquitination of DAPK, we monitored the

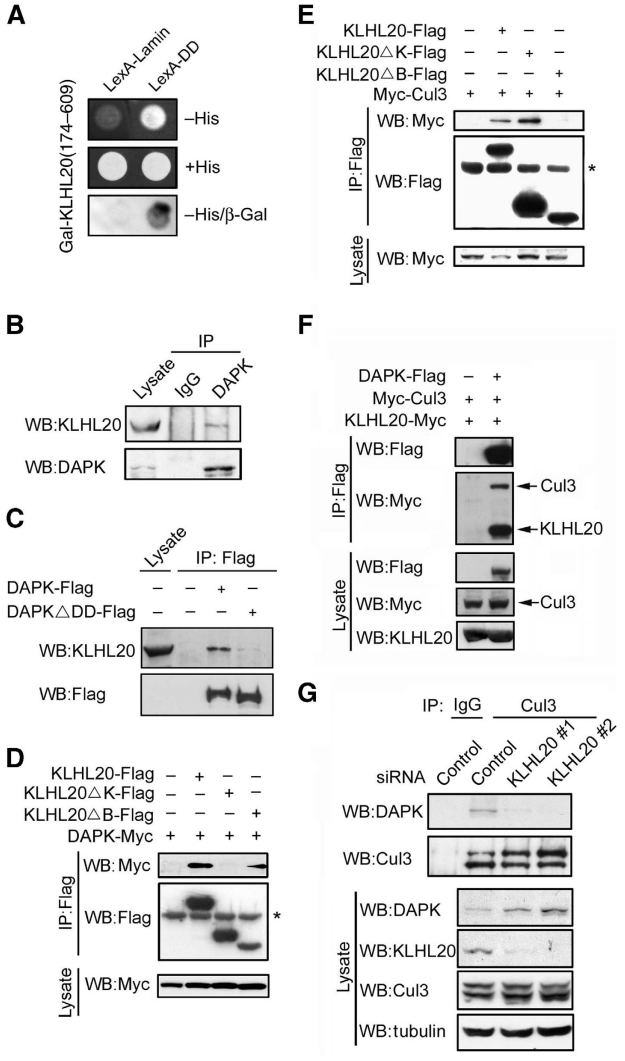

Figure 1 Interaction of KLHL20 with Cul3 and DAPK. (**A**) Identification of KLHL20 as a DAPK-binding protein. Yeast strain L40 contransformed with Gal- and LexA-based constructs as indicated was assayed for His3 phenotype (−His) or β-galactosidase activity (β-Gal). (**B**) Endogenous KLHL20 interacts with endogenous DAPK. Lysates of HeLa cells were used for immunoprecipitation with anti-DAPK antibody or control IgG and the immunoprecipitates and cell lysate were subjected to western blot with antibodies as indicated. (**C**) The DD of DAPK is involved in binding KLHL20. Lysates of 293T cells transfected with DAPK-Flag or DAPKΔDD-Flag were used for immunoprecipitation and western blot analyses with antibodies as indicated. (**D**, **E**) Mapping the KLHL20 domain responsible for binding DAPK (**D**) or Cul3 (**E**). 293T cells were cotransfected with various constructs as indicated. Cells were lysed for immunoprecipitation and western blot analyses with antibodies as indicated. The position of immunoglobulin heavy chain is marked with an asterisk. (**F**) Cul3 coprecipitates with DAPK. Lysates of 293T cells cotransfected with various constructs were analysed by immunoprecipitation and/or western blot with indicated antibodies. (**G**) KLHL20 mediates the interaction between DAPK and Cul3. HeLa cells were infected with lentivirus carrying indicated siRNA and then selected with puromycin. The resulting stable knockdown cells were analysed by immunoprecipitation followed by western blot with antibodies as indicated. KLHL20, Cul3, and DAPK expression levels were assayed by western blot (bottom panel).

DAPK ubiquitination levels in cells transfected with KLHL20, Cul3, and/or ROC1. Although DAPK polyubiquitination was readily detected in the absence of ectopic KLHL20 and Cul3, cotransfection of ROC1, KLHL20, and Cul3 together led to a great induction of DAPK polyubiquitination. Omission of either Cul3 or KLHL20 reduced DAPK ubiquitination level (Figure 2A). Importantly, the ROC1–Cul3–KLHL20-mediated DAPK ubiquitination was abolished by deleting either the ROC1-binding site (amino acid 597–615) in Cul3 (Cul3ΔR) or the DAPK-binding domain in KLHL20 (KLHL20ΔK) (Figure 2B, left). Furthermore, we generated a KLHL20 mutant (KLHL20m6), in which each of the six residues corresponding to those in Skp1 contacting Cul1 predicted by structural modelling (Supplementary Figure S4A) was replaced by an alanine. This mutant, which was defective in Cul3 binding (Supplementary Figure S4B), could no longer support Cul3-mediated DAPK ubiquitination (Figure 2B, right). Finally, we found that the ROC1–Cul3–KLHL20 complex could not efficiently promote the ubiquitination of DAPKΔDD mutant (Figure 2C), consistent with the defect of this mutant in binding KLHL20. Together, these results indicate that an intact ROC1–Cul3–KLHL20 complex and an efficient interaction between DAPK and KLHL20 are important for DAPK ubiquitination *in vivo*.

To determine the function of endogenous KLHL20 in DAPK ubiquitination, we used the aforementioned HeLa cell derivatives carrying control siRNA or KLHL20 siRNAs. In cells expressing either of the two KLHL20 siRNAs, DAPK ubiquitination was markedly diminished, and the extent of decrease in DAPK ubiquitination correlated with the efficiency of KLHL20 depletion (comparing Figures 2D with 1G). Next, we tested whether the ROC1–Cul3–KLHL20 complex would be sufficient to trigger DAPK ubiquitination *in vitro*. To this end, 293T cells were transfected with constructs-expressing GST-Cul3, Myc-KLHL20, and Myc-ROC1, and then the ROC1–Cul3–KLHL20 complex was purified by Glutathione Sepharose (Supplementary Figure S5). This complex was then incubated with purified, baculovirally expressed Flag-DAPK in the *in vitro* ubiquitination reaction. Western blot analysis of the reaction mixture with anti-Flag antibody detected a high-molecular-weight smear, representing the polyubiquitinated DAPK (Figure 2E). Omission of ubiquitin, E1/E2, or the ROC1–Cul3–KLHL20 complex from the reaction prevented DAPK polyubiquitination. Furthermore, replacement of wild-type Cul3 with the Cul3ΔC mutant (Cul3 1–199) or wild-type KLHL20 with the KLHL20m6 mutant impaired the formation of intact ROC–Cul3–KLHL20 complex (Supplementary Figure S5) and compromised DAPK ubiquitination *in vitro* (Figure 2F). Together, these data provide compelling evidence that DAPK is a direct substrate of the ROC1–Cul3–KLHL20 E3 ligase.

KLHL20 promotes DAPK proteasomal degradation and attenuates its proapoptotic function

The ability of KLHL20 to target DAPK for Cul3-mediated polyubiquitination suggests its function in promoting DAPK proteasomal degradation. Indeed, overexpression of KLHL20 decreased the steady-state levels of both ectopic and endogenous DAPK, and this effect of KLHL20 was reversed by the proteasome inhibitor MG132 (Figure 3A). The KLHL20ΔK and KLHL20m6 mutants, however, failed to affect DAPK level. KLHL20 overexpression also accelerated DAPK turnover, as revealed by the cycloheximide-chase treatment (Figure 3B). Furthermore, depletion of KLHL20 led to an accumulation of endogenous DAPK (Figures 1G and 3C),

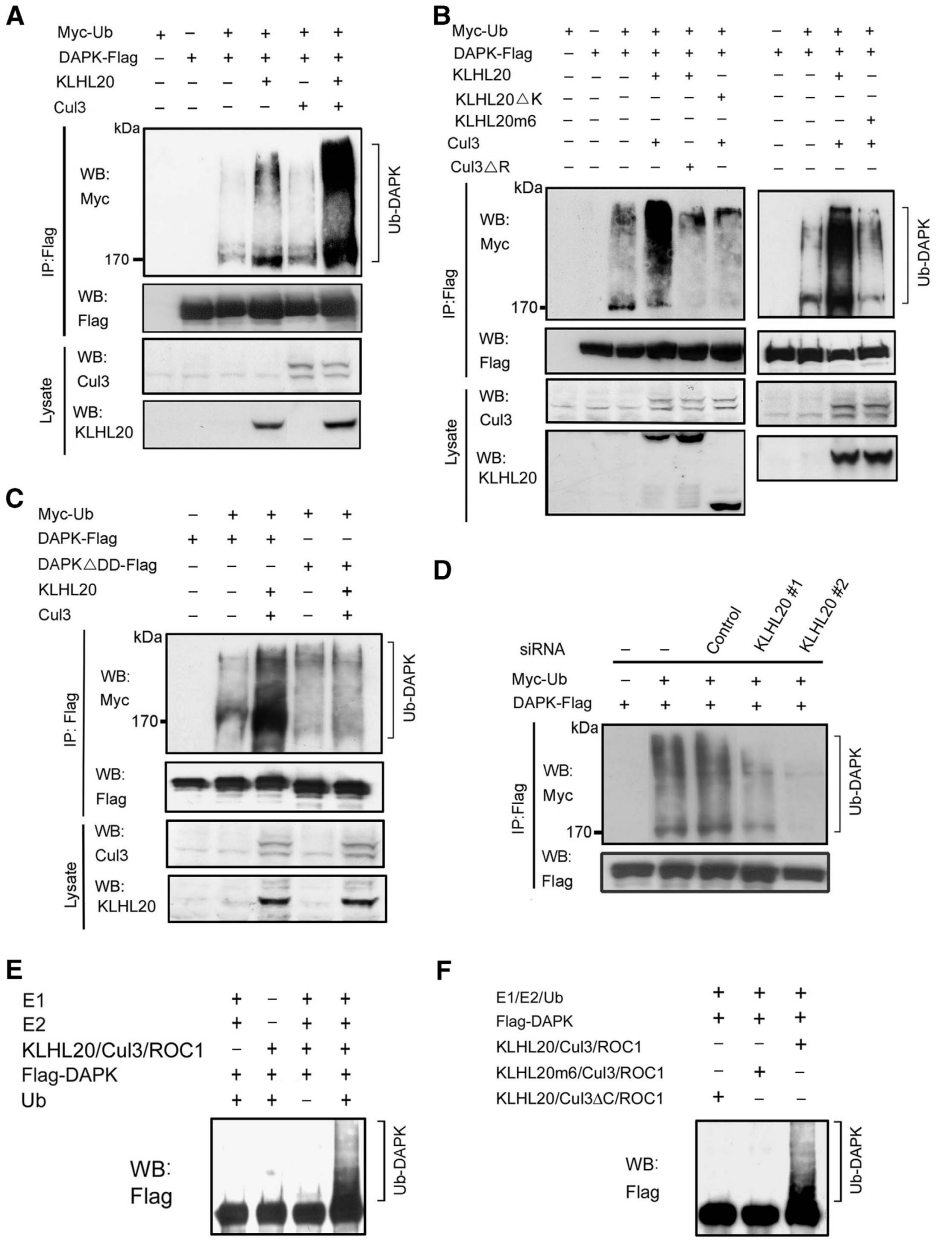

Figure 2 KLHL20–Cul3–ROC1 complex is a ubiquitin ligase for DAPK. (**A**, **B**) KLHL20–Cul3–ROC1 complex promotes DAPK ubiquitination *in vivo*. 293T cells were transfected with constructs expressing Myc-ubiquitin (Myc-Ub), ROC1 (not indicated), Cul3 (or mutant), KLHL20 (or mutant), and/or DAPK-Flag and treated with MG132 for 16 h. Cell lysates were used to detect DAPK ubiquitination by immunoprecipitation with anti-Flag antibody, followed by western blot with anti-Myc antibody. The expression levels of Cul3 and KLHL20 were examined by western blot (bottom panel). (**C**) The DD of DAPK is important for DAPK ubiquitination by KLHL20–Cul3–ROC1 complex. 293T cells transfected with indicated constructs and treated with MG132 were assayed for DAPK ubiquitination as in (**A**). (**D**) Endogenous KLHL20 promotes DAPK ubiquitination. HeLa cell derivatives as in Figure 1G were transfected with Myc-Ub and/or DAPK-Flag and assayed for DAPK ubiquitination as in (**A**). (**E**–**F**) *In vitro* ubiquitination of DAPK by the KLHL20–Cul3–ROC1 E3 ligase. Cul3 complex was purified by Glutathione Sepharose from lysates of 293T cells transfected with GST-Cul3 (or its mutant), Myc-ROC1, and KLHL20-Myc (or its mutant). The copurification of ROC1 and/or KLHL20 with GST-Cul3 was shown in Supplementary Figure S5. The Cul3 complex was subjected to *in vitro* ubiquitination assay in the presence of E1, E2, ubiquitin, and/or Flag-DAPK purified from baculovirus (see Materials and methods). The reaction was resolved on SDS–PAGE and analysed by western blot with anti-Flag antibody.

thus showing the ability of endogenous KLHL20 to regulate endogenous DAPK. Consistent with its ability to downregulate DAPK expression, KLHL20 overexpression attenuated apoptosis induced by wild-type DAPK or its active mutant (ΔCaM), whereas KLHL20ΔK did not affect this proapoptotic activity (Figure 3D). These findings indicate that KLHL20 downregulates DAPK protein level and biological function by promoting DAPK ubiquitination.

IFN-α and IFN-γ inhibit KLHL20-dependent DAPK ubiquitination by sequestration of KLHL20

Next, we explored whether KLHL20-dependent DAPK ubiquitination could be regulated in response to a physiological stimulus. By screening a number of death stimuli, we observed that IFN-γ induced a substantial increase in the protein levels of both overexpressed (Figure 4A) and endogenous (Figure 4B) DAPK. Intriguingly, although MG132

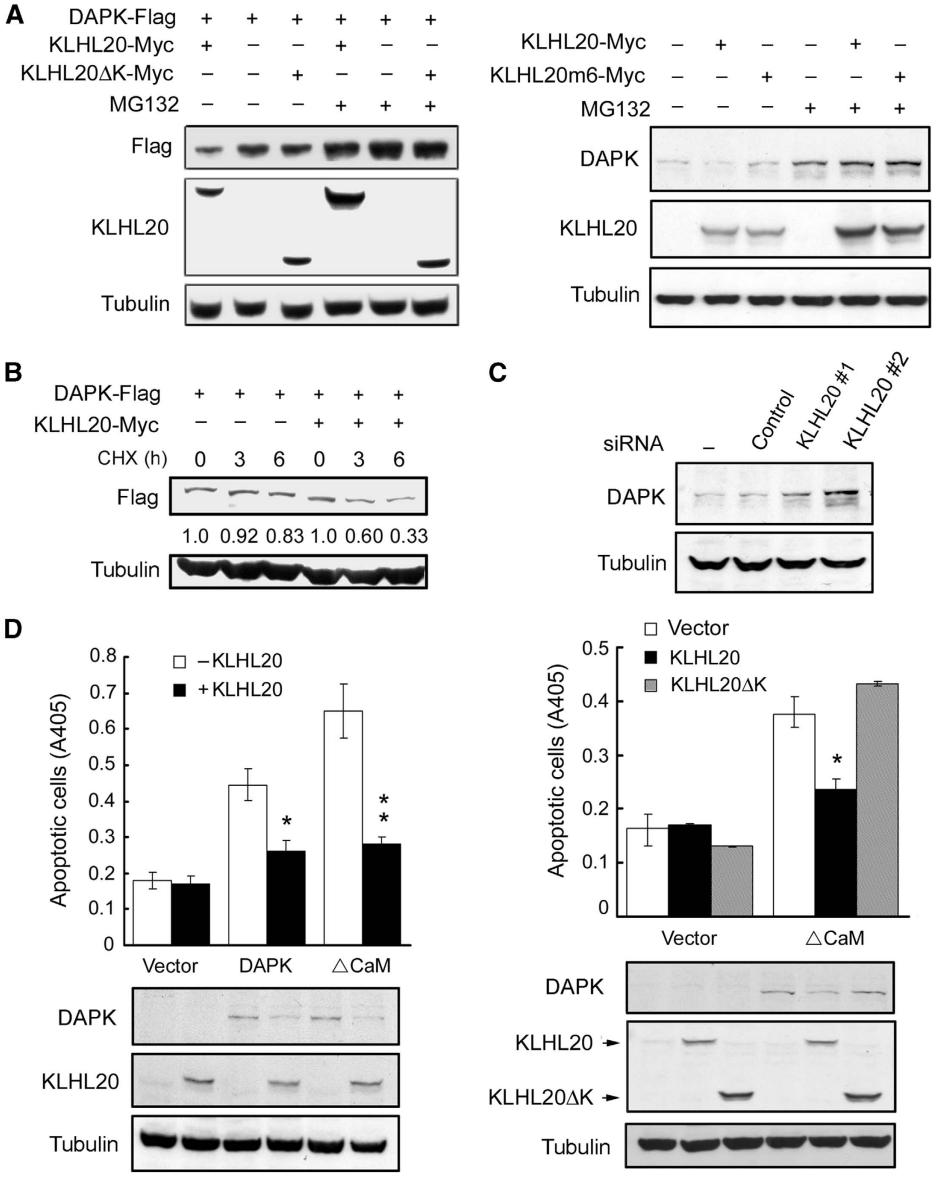

Figure 3 KLHL20 enhances DAPK proteasomal degradation and attenuates DAPK proapoptotic activity. (**A**) KLHL20 promotes proteasomal degradation of DAPK. 293T cells transfected with indicated constructs were treated with 1 μM MG132 or DMSO (−) for 12 h, and then lysed for western blot analyses. (**B**) KLHL20 promotes DAPK turnover. HeLa cells transfected with indicated constructs were treated with 100 μg/ml cycloheximide for various time points before lysis. Cell lysates were analysed by western blot. The amounts of Flag-DAPK relative to that of untreated cells are indicated. (**C**) Knockdown of KLHL20 increases DAPK steady-state level. HeLa cell derivatives as in Figure 1G were analysed for DAPK level by western blot. (**D**) KLHL20 inhibits the proapoptotic function of DAPK. NIH3T3 cells were transiently transfected with DAPK (or DAPKΔCaM) together with or without KLHL20 (or KLHL20ΔK). Apoptosis was assayed by the Cell Death Detection ELISA kit. Data are represented as mean ± s.e.m. (*$P<0.05$; **$P<0.005$; $n=3$). The expression levels of various proteins are shown on the bottom panel.

treatment resulted in an elevation of DAPK level in cells without receiving IFN-γ, it did not significantly upregulate DAPK in IFN-γ-treated cells (Figure 4B). These findings suggest that IFN-γ stabilizes DAPK by inhibiting its proteasomal degradation. A similar DAPK stabilization was observed in IFN-α-treated cells (Figure 4B). We then tested the underlying mechanism of this DAPK stabilization. Both IFN-γ and IFN-α led to a marked inhibition of DAPK ubiquitination induced by KLHL20 and Cul3 (Figure 4C and D). Although the formation of ROC1–Cul3–KLHL20 E3 ligase complex was not affected (Supplementary Figure S6), KLHL20 interaction with endogenous DAPK was blocked in response to IFN-γ (Figure 5A). In correlating with the dissociation of KLHL20–DAPK complex, a drastic alteration in the subcellular localization of KLHL20 was detected in IFN-γ-treated cells (Figure 5B, upper panel). In the absence of IFN-γ, KLHL20 was concentrated in the perinuclear region and dispersed in the remaining cytoplasm. In addition, a small fraction of KLHL20 was found in the nucleus, particularly, PML-NBs (Figure 5B, magnified image shown in the inset). On IFN-γ treatment, KLHL20 was enriched in PML-NBs, which occurred simultaneously with an increase of both size and number of PML-NBs. The distribution of KLHL20 in the cytoplasm was significantly reduced in this circumstance. DAPK, however, was mainly localized in the cytoplasm and this localization was not affected by IFN-γ (Figure 5B, lower

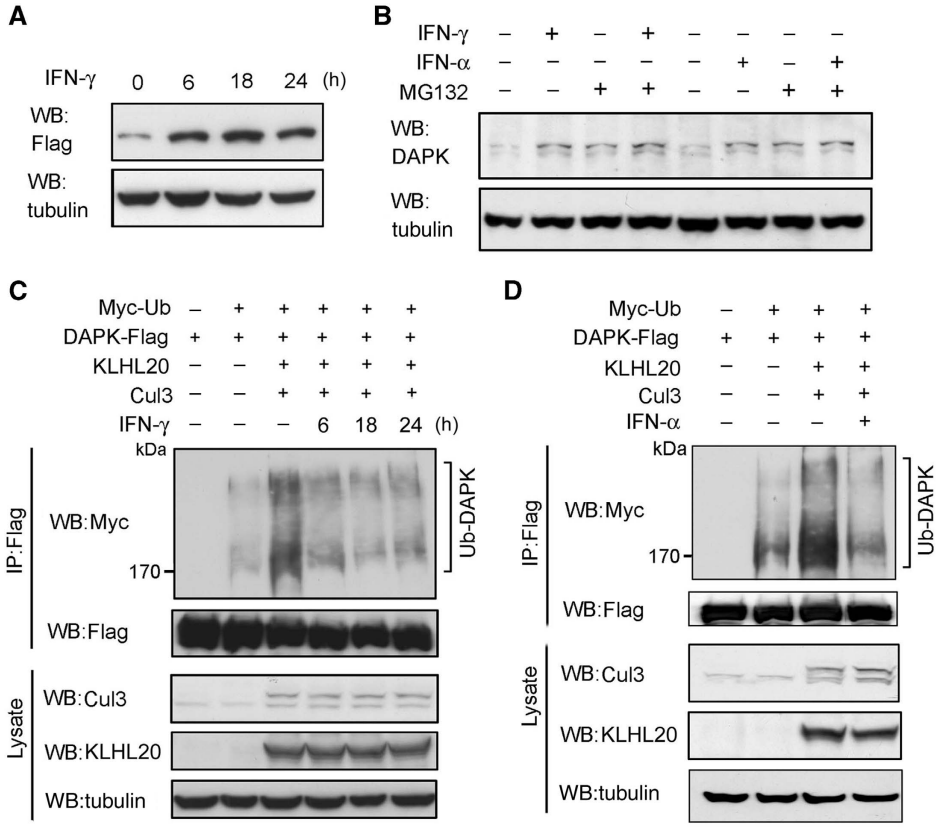

Figure 4 IFN blocks KLHL20-dependent DAPK ubiquitination and degradation. (**A**) IFN upregulates DAPK. 293T cells transfected with DAPK-Flag were treated with 1000 U/ml IFN-γ for indicated time points and then lysed for western blot analysis. (**B**) IFN inhibits proteasomal degradation of DAPK. HeLa cells were treated with 1500 U/ml IFN-α or 1000 U/ml IFN-γ for 18 h and then with 30 μM MG132 (or DMSO) for 3 h. The level of endogenous DAPK was analysed by western blot. (**C**, **D**) IFN-α or IFN-γ blocks KLHL20-dependent DAPK ubiquitination. 293T cells were transfected with Myc-Ub, Cul3, ROC1, KLHL20, and/or DAPK-Flag. Two days after transfection, cells were treated with IFN-γ for indicated time points (**C**) or IFN-α for 18 h (**D**). DAPK ubiquitination was assayed as in Figure 2A.

panel). A similar enrichment of KLHL20 in PML-NBs was observed in IFN-α-treated cells (Supplementary Figure S7). These intriguing findings thus suggest that both IFN-α and IFN-γ induce a spatial separation of KLHL20 from its substrate DAPK. As these IFNs are known to transcriptionally induce PML expression (Lavau *et al*, 1995; Stadler *et al*, 1995), we reasoned that the IFN-α/γ-triggered enrichment of KLHL20 in PML-NBs may be the result of a physical interaction between KLHL20 and PML. Accordingly, immunoprecipitation analysis showed a coprecipitation of endogenous PML with KLHL20. Notably, a higher amount of PML was coprecipitated with KLHL20 from lysate of IFN-γ-treated cells (Figure 5C, upper panel), correlating with the increased PML expression level (Figure 5C, lower panel). We further found that the interaction between KLHL20 and DAPK was disrupted by overexpressing PML-I (Figure 5D, upper panel), the longest and abundantly expressed PML isoform. Conversely, KLHL20 interaction with endogenous PML was blocked by overexpressing DAPK (Figure 5D, lower panel). In addition, pull down analysis showed that PML and DAPK competed for binding KLHL20 *in vitro* (Supplementary Figure S8). Together, our data support a model in which IFN-α/γ-induced PML recruits a significant amount of KLHL20 to PML-NBs through their physical interaction. This relocation of KLHL20 results in a spatial separation of KLHL20 from DAPK, thereby blocking KLHL20-dependent DAPK ubiquitination and proteasomal degradation. As IFN-γ and IFN-α have similar effects on KLHL20 subcellular localization and KLHL20-mediated DAPK ubiquitination, we used only one of the agents in subsequent studies.

PML depletion reverses the inhibitory effect of IFN on DAPK ubiquitination and degradation

If the recruitment of KLHL20 to PML-NBs indeed accounts for the blockage of KLHL20-mediated DAPK ubiquitination in IFN-α/γ-treated cells, depletion of PML should reverse this effect. To test this possibility, we used two PML siRNAs to downregulate PML expression in HeLa cells. Both PML siRNAs are designed to target the RBCC region of PML, and therefore are expected to knockdown all PML isoforms. Expression of PML siRNA, but not control siRNA, greatly reduced PML protein level, which was most evident in IFN-γ-treated conditions (Figure 6A). Furthermore, the IFN-γ-induced formation of PML-NBs was greatly inhibited in PML siRNA-expressing cells, and thus IFN-γ failed to alter the subcellular localization of KLHL20 (Supplementary Figure S9). As a result, in cells expressing PML siRNA, but not control siRNA, IFN-γ could no longer induce the dissociation of KLHL20–DAPK complex (Figure 6B), thus restoring the KLHL20-dependent DAPK ubiquitination (Figure 6C). Consequently, the IFN-γ-induced DAPK upregulation was completely blocked by PML depletion (Figure 6B, bottom

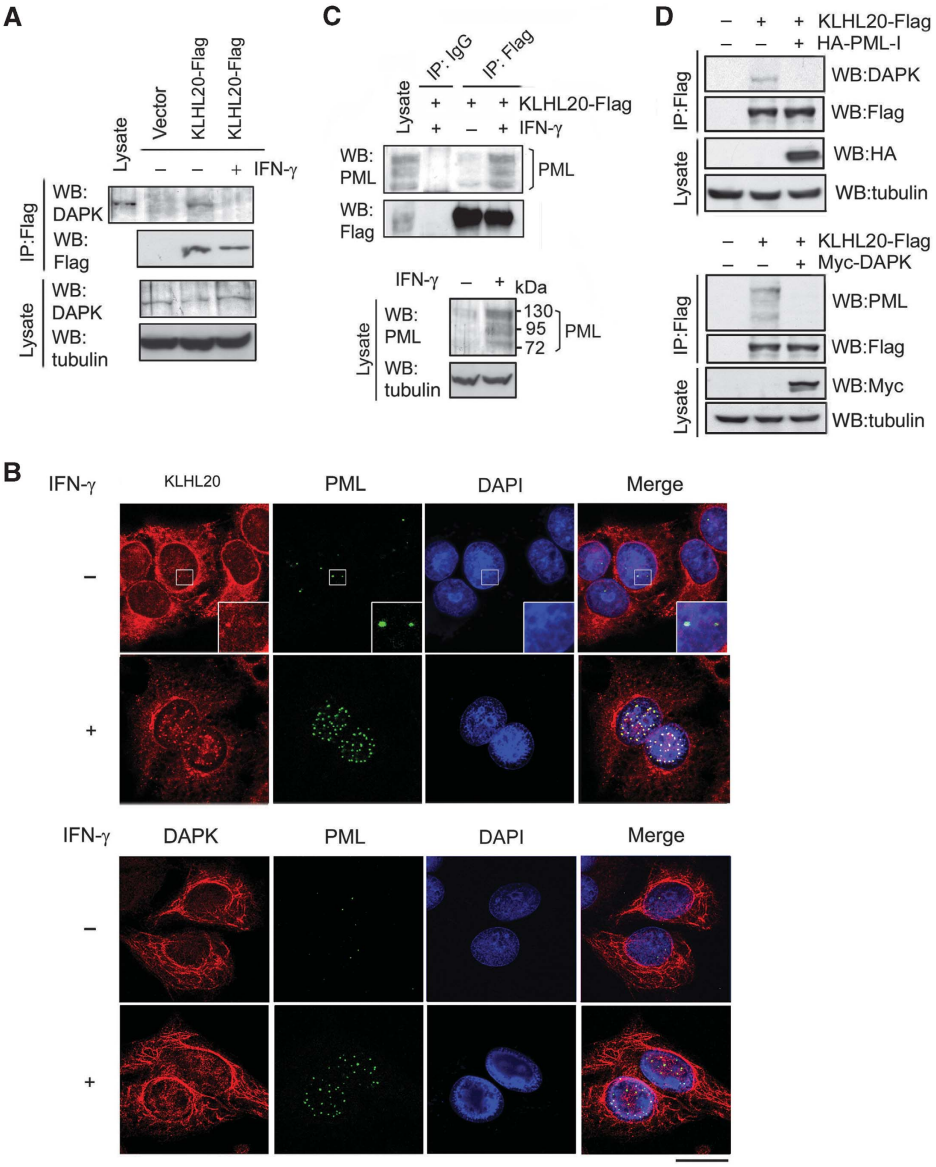

Figure 5 IFN triggers the disruption of KLHL20–DAPK complex by sequestrating KLHL20 in PML-NBs. (**A**) IFN blocks the interaction of KLHL20 with endogenous DAPK. HeLa cells transfected with KLHL20-Flag were treated with IFN-γ for 18 h and lysed for immunoprecipitation with anti-Flag antibody. The immunoprecipitates and cell lysates were analysed by western blot with indicated antibodies. (**B**) IFN triggers the enrichment of KLHL20 in PML-NBs. HeLa cells were treated with or without IFN-γ for 18 h. Cells were fixed, triple stained by DAPI, anti-KLHL20 antibody and anti-PML antibody (upper panel) or by DAPI, anti-DAPK antibody and anti-PML antibody (bottom panel), and examined by confocal microscopy. The box area was amplified to show the colocalization of KLHL20 and PML. Bar, 20 μm. (**C**) Interaction of KLHL20 with PML. HeLa cells transfected and treated as in (**A**) were lysed for immunoprecipitation with anti-Flag or a control antibody (IgG). The immunoprecipitates and cell lysates were analysed by western blot with antibodies as indicated. (**D**) DAPK and PML compete for binding KLHL20. 293T cells transfected with indicated constructs were subjected to immunoprecipitation with anti-Flag, followed by western blot with indicated antibodies.

panel). To further confirm the critical function of PML in IFN-γ-induced DAPK stabilization, we used the PML null mouse embryonic fibroblasts (MEFs) and their wild-type counterparts. Although IFN-γ robustly induced DAPK steady-state level in wild-type MEFs, this effect was not observed in $PML^{-/-}$ MEFs (Figure 6D). Similarly, cycloheximide experiment revealed that the DAPK stabilization effect of IFN-γ was completely abrogated in $PML^{-/-}$ MEFs (Figure 6E). Together, these results provide substantial evidence that PML-mediated sequestration of KLHL20 in PML-NBs is essential for the blockage of KLHL20-dependent DAPK ubiquitination and degradation under IFN-treated conditions.

DAPK stabilization by blocking KLHL20-mediated ubiquitination contributes to IFN-α-induced apoptosis in multiple myeloma cells

DAPK was originally identified by its involvement in IFN-induced cell death (Deiss *et al*, 1995). The uncovering of IFN-induced DAPK stabilization prompted us to investigate the contribution of this event to IFN-induced apoptosis. Importantly, earlier studies revealed a tight correlation between induction of PML and IFN-α sensitivity of human tumors, such as multiple myeloma (MM) and hepatocelluar carcinoma (Crowder *et al*, 2005; Herzer *et al*, 2009). On the basis of these earlier reports and our current study, we

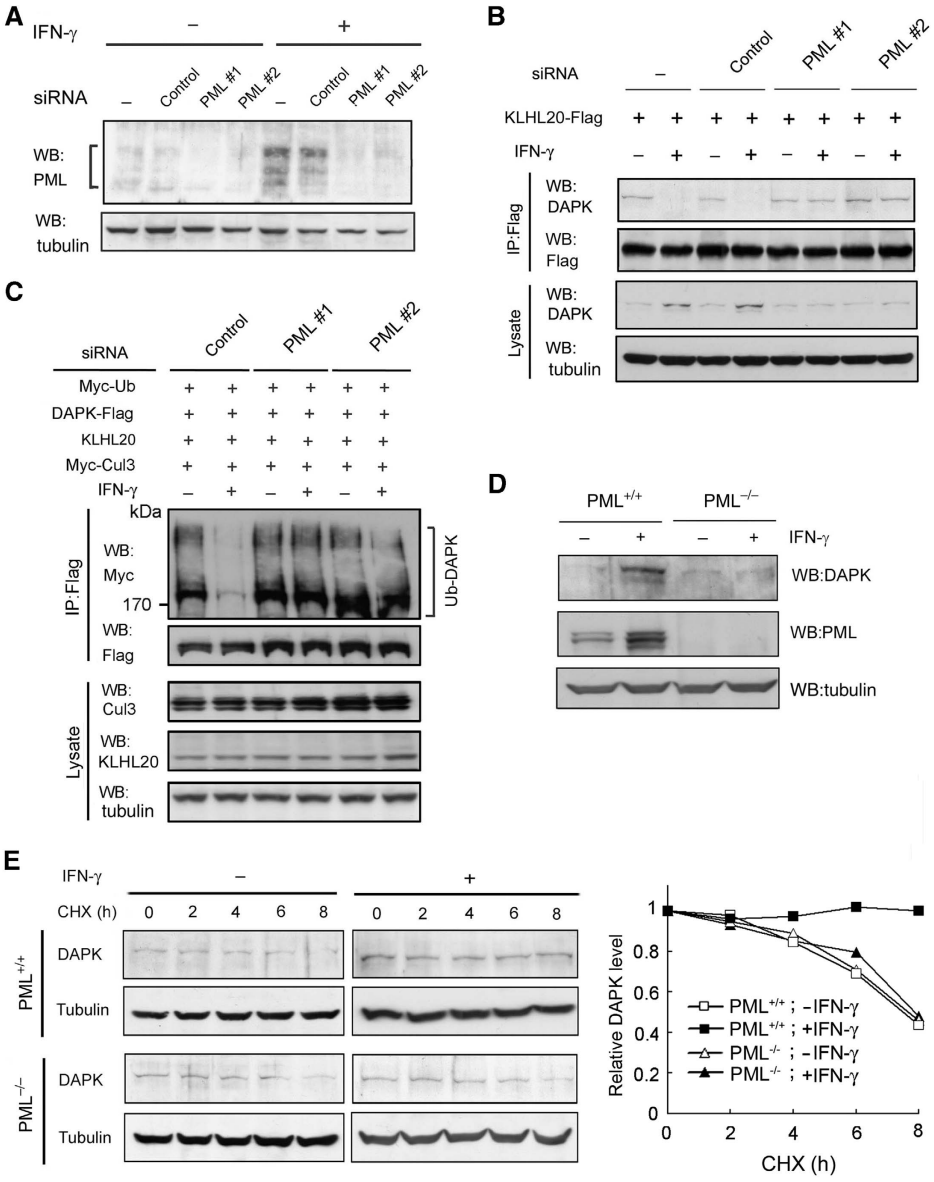

Figure 6 PML depletion reverses the inhibitory effects of IFN on DAPK ubiquitination and degradation. (**A**) Generation of PML knockdown cells. HeLa cells were infected with lentivirus carrying indicated siRNA and selected with puromycin. Cells were treated with or without IFN-γ for 18 h and then lysed for western blot analysis. (**B**) PML siRNA rescues the interaction between DAPK and KLHL20 in IFN-γ-treated cells. Cells as in (**A**) were transfected with KLHL20-Flag and treated with IFN-γ for 18 h. Cells were lysed for immunoprecipitation with anti-Flag antibody. The immunoprecipitates and cell lysates were analysed by western blot with antibodies as indicated. (**C**) PML siRNA rescues KLHL20-mediated DAPK ubiquitination in IFN-γ-treated cells. Cells as in (**A**) were transfected with indicated constructs and treated with IFN-γ for 18 h. DAPK ubiquitination was analysed as in Figure 2A. The expression levels of various proteins are shown on the bottom. (**D**) IFN-γ fails to upregulate DAPK in PML null cells. $PML^{+/+}$ or $PML^{-/-}$ MEFs were treated with IFN-γ for 18 h and then lysed for western blot analysis with indicated antibodies. (**E**) PML is required for IFN-γ-induced DAPK stabilization. Cells as in (**D**) were treated with IFN-γ for 18 h and then with 50 μg/ml cycloheximide for indicated time points. Cells were lysed for western blot analysis and the level of DAPK was normalized to that of tubulin and plotted on the right.

hypothesized that the capability of blocking KLHL20-mediated DAPK degradation governs the fate of these tumors in response to IFN-α treatment. To test this hypothesis, we used a pair of MM cell lines: the IFN-sensitive H929 cells and the IFN-resistant XG1 cells. In agreement with one earlier report (Crowder *et al*, 2005), IFN-α treatment led to a significant induction of PML-NBs in H929 but not XG1 cells (Figure 7A and B). As a result, enrichment of KLHL20 in PML-NBs (Figure 7A and B), disruption of DAPK–KLHL20 complex (Figure 7C), and upregulation of DAPK (Figure 7D) after IFN-α treatment were evident in H929 but not in XG1 cells. We expected that this blockage of KLHL20-mediated DAPK degradation and subsequent accumulation of proapoptotic DAPK would contribute to the IFN sensitivity of H929 cells. Consistent with this notion, the responsiveness of H929 cells to IFN-α was greatly suppressed by either depleting DAPK or overexpressing KLHL20 (Figure 7E, upper panel). KLHL20m6, however, failed to inhibit IFN-α-induced apoptosis, suggesting that the formation of Cul3–KLHL20 complex is important for the antiapoptotic effect of KLHL20. Importantly, overexpression of a KLHL20-resistant DAPKΔDD mutant completely reversed the effect of KLHL20 on

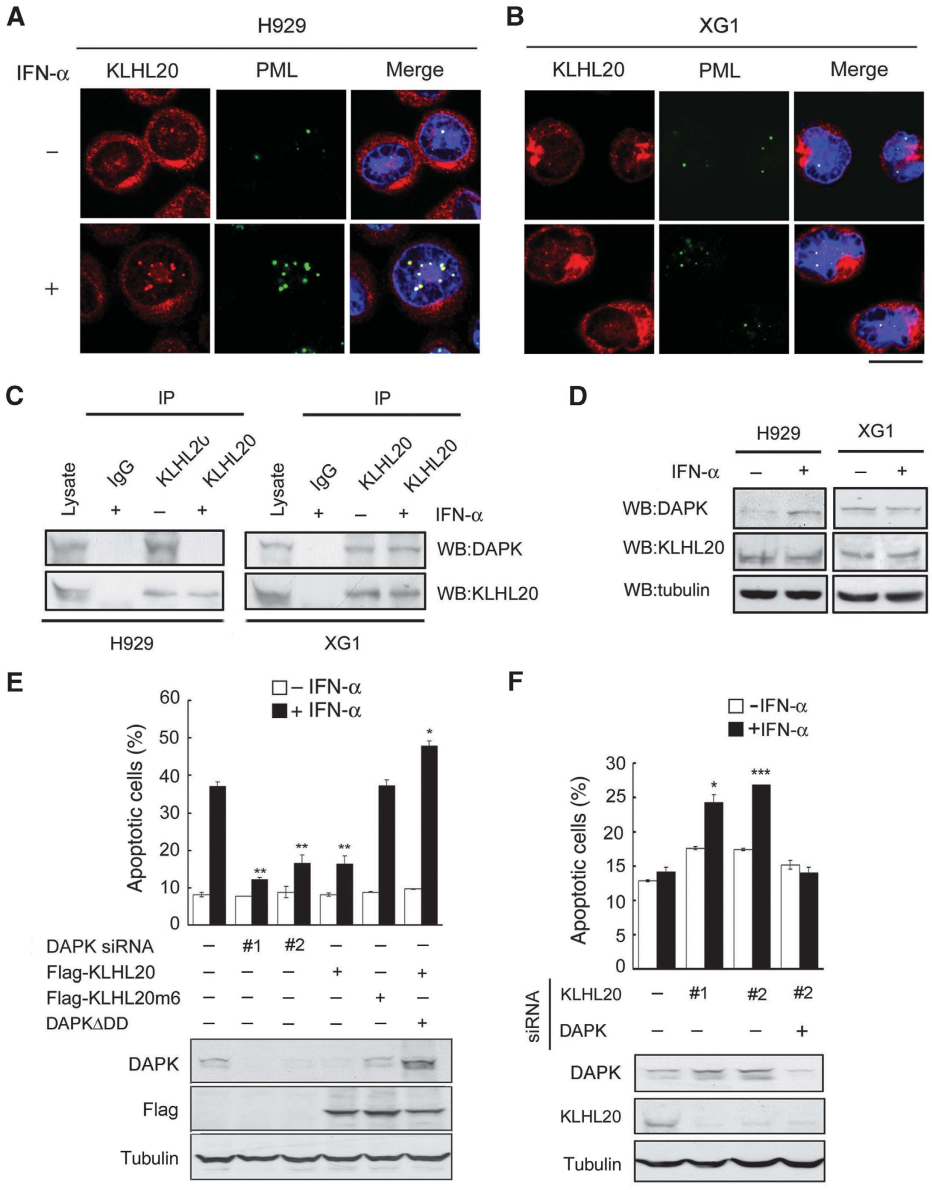

Figure 7 Blockage of KLHL20-mediated DAPK degradation contributes to MM cell responsiveness to IFN. (**A**, **B**) IFN-α induces PML-NBs and KLHL20 relocation in H929 cells but not in XG1 cells. Cells treated with IFN-α (1000 U/ml) for 16 h were fixed, stained by DAPI (blue), anti-KLHL20 antibody and anti-PML antibody, and examined by confocal microscopy. Bar, 10 μm. (**C**) IFN-α induces the disruption of KLHL20–DAPK complex in H929 cells but not in XG1 cells. Cells as indicated were treated as in (**A**) and then subjected to immunoprecipitation with anti-KLHL20 antibody or control antibody (IgG), followed by western blot with anti-KLHL20 or anti-DAPK antibody. (**D**) IFN-α induces the upregulation of DAPK in H929 cells but not in XG1 cells. Cells treated as in (**A**) were analysed by western blot with antibodies as indicated. (**E**) H929 cells were infected with lentivirus-expressing KLHL20, KLHL20m6 or DAPK siRNA and then selected with blasticidin (for KLHL20 construct) or puromycin (for siDAPK construct). To generate cells stably expressing both KLHL20 and DAPKΔDD, H929 cells were first infected with retrovirus carrying DAPKΔDD and selected with puromycin. The resulting stable line was then infected with lentivirus-expressing KLHL20 and selected with blasticidin. Cell lysates were analysed by western blot with antibodies as indicated (bottom panel). Alternatively, cells were treated with IFN-α and apoptosis was assayed by Annexin V staining followed by flow cytometry analysis (upper panel). (**F**) XG1 cells were infected with lentivirus carrying indicated siRNAs and then selected with hygromycin (for DAPK siRNA construct) and/or puromycin (for KLHL20 siRNA construct). Cells were lysed for western blot analysis (bottom panel). Alternatively, IFN-α-induced apoptosis was assayed as in (**C**). Data are represented as mean ± s.e.m. ($*P<0.05$; $**P<0.005$; $***P<0.0005$; $n=3$).

IFN-α-induced apoptosis, even though this mutant is known to elicit a weaker proapoptotic activity than its wild-type counterpart (Chen *et al*, 2005). Furthermore, in all H929 derivatives, the IFN sensitivity correlated tightly with DAPK level (Figure 7E, bottom panel). These results collectively support a critical function of suppressing KLHL20-mediated DAPK degradation in IFN-α-induced apoptosis. To further confirm this notion, we turned to XG1 cells. We postulated that DAPK may be persistently degraded by KLHL20 in this cell line due to a failure of IFN-α to induce PML-NBs. To address whether this effect could account for the IFN-resistant feature of XG1 cells, we depleted KLHL20 using two different siRNAs. Importantly, both siRNAs made XG1 cells responsive to IFN (Figure 7F, upper panel). To address whether this effect of KLHL20 siRNAs was mediated by DAPK upregulation (Figure 7F, bottom panel), we depleted

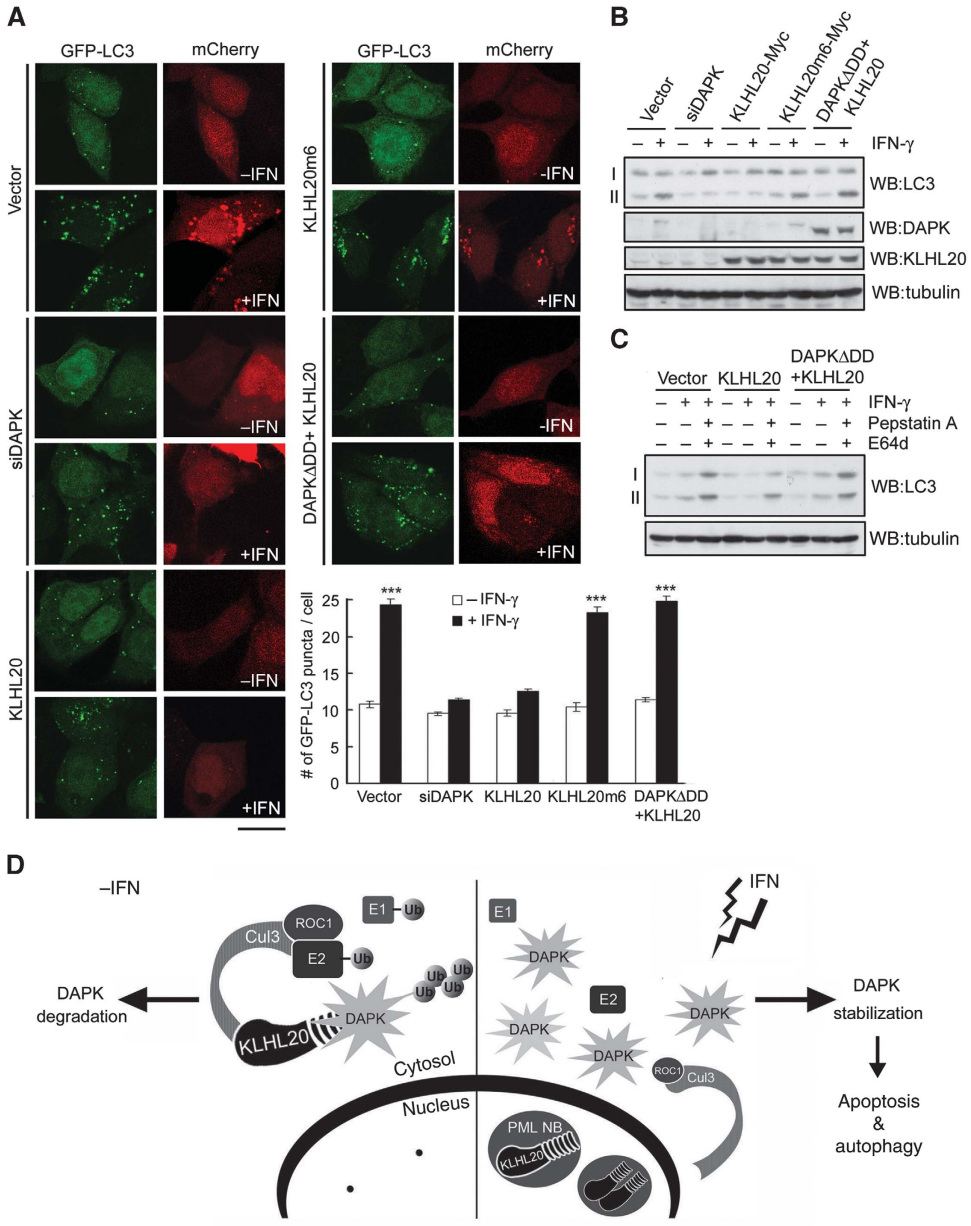

Figure 8 Blockage of KLHL20-mediated DAPK degradation contributes to IFN-induced autophagy. (**A**) MCF7-LC3 cells were transfected with various constructs together with mCherry-expressing construct and then treated with or without IFN-γ. The GFP-LC3 signal was examined by confocal microscopy (for image presentation) and epifluorescent microscopy (for quantification). Bar, 20 μm. The number of GFP-LC3 dots per cell was quantified from 50 mCherry-positive cells and plotted (bottom panel). Data are represented as mean ± s.e.m. (***$P<0.0005$; $n=3$). (**B**) MCF7 parental cells were transfected and treated as in (**A**) and then analysed by western blot with indicated antibodies. The positions of LC3-I and LC3-II are indicated. (**C**) MCF7 cells transfected and treated as in (**B**) except for the addition of E64d and pepstatin A at 16 h before harvest. Cell lysates were analysed by western blot with antibodies as indicated. (**D**) Models for the DAPK degradation pathway mediated by KLHL20–Cul3–ROC1 E3 ligase complex and for the inhibition of this pathway in IFN-treated cells.

DAPK in KLHL20-knockdown cells. Indeed, IFN resistance was restored in the double knockdown cells. Thus, our findings not only show that DAPK acts as a downstream effector of PML in IFN-induced apoptosis, but also indicate that the KLHL20-mediated DAPK degradation has a determining function in IFN responsiveness of tumor cells.

Inhibition of KLHL20-mediated DAPK ubiquitination contributes to IFN-induced autophagy

IFN is known to trigger apoptotic or autophagic death depending on cell context. As DAPK is also a critical mediator of IFN-induced autophagy (Inbal *et al*, 2002), we investigated whether blockage of KLHL20-mediated DAPK ubiquitination could contribute to autophagy induction by IFN. To this end, we used the MCF7 cell line, in which DAPK has a positive function in autophagy induction (Inbal *et al*, 2002). Furthermore, the inhibitory effect of IFN-γ on KLHL20-mediated DAPK degradation could be recapitulated in this cell line, as evident the enrichment of KLHL20 in PML-NBs (Supplementary Figure S10) and the upregulation of DAPK (Figure 8B) under IFN-γ-treated conditions. To monitor the formation of autophagosome, MCF7 cells stably expressing the autophagosome-associated marker GFP-LC3 were established. After IFN-γ treatment, a prominent induction of

LC3-positive autophagic vesicles was observed (Figure 8A). Consistent with an earlier study (Inbal *et al*, 2002), this induction of autophagosome was attenuated by depleting DAPK. Importantly, overexpression of KLHL20, but not KLHL20m6, similarly blocked IFN-induced LC3 puncta, and this effect was reversed by coexpression of KLHL20 with DAPKΔDD. To further assess the effect of KLHL20-mediated DAPK degradation on IFN-induced autophagy, we monitored the conversion of LC3 from cytosolic form (LC3-I) to its autophagosome-associated form (LC3-II) in the parental MCF7 cells. As shown in Figure 8B, IFN-γ treatment led to a marked increase of LC3-II level, which was abrogated by depleting DAPK or overexpressing KLHL20, but not by overexpressing KLHL20m6. Coexpression of KLHL20 and DAPKΔDD again reversed the inhibitory effect of KLHL20 on LC3-II production. Of note, the increased GFP-LC3 puncta and LC3-II production seen in Figure 8A and B, respectively, were resulted from the increase in autophagosome formation rather than the blockage of lysosome-mediated autophagic flux, as treatment of lysosome inhibitors E64d and pepstatin A further elevated the level of LC3-II (Figure 8C). Together, these results indicate that blockage of KLHL20-mediated DAPK ubiquitination contributes to the autophagy-induction effect of IFN.

Discussion

In this study, we show that KLHL20 negatively regulates DAPK by targeting it to the Cul3–ROC1 complex for ubiquitination, which in turn triggers the proteasomal degradation of DAPK (Figure 8D, left panel). Several lines of evidence support this conclusion. First, KLHL20 binds DAPK through the Kelch-repeat domain and Cul3 through the BTB domain, consistent with its function as a substrate adaptor to bridge DAPK to the Cul3–ROC1 ligase. Second, an intact ROC1–Cul3–KLHL20 complex is critical for DAPK ubiquitination *in vivo* and disruption of either Cul3–ROC1 or Cul3–KLHL20 interaction abrogates this ubiquitination activity. Third, DAPK mutant that cannot efficiently bind KLHL20 displays a significant impairment of ubiquitination by KLHL20-based E3 ligase, suggesting a direct action of this ligase on DAPK. Accordingly, affinity-purified ROC1–Cul3–KLHL20 complex is capable of inducing DAPK polyubiquitination *in vitro*. Finally, siRNA-mediated depletion of endogenous KLHL20 leads to an inhibition of DAPK ubiquitination and an accumulation of DAPK protein. Thus, our study establishes an important and physiological function of ROC1–Cul3–KLHL20 in DAPK ubiquitination.

When searching for an upstream signal that could regulate the KLHL20-mediated DAPK ubiquitination, we observed that the administration of IFN-α or IFN-γ drastically blocks this ubiquitination event through disrupting the interaction between DAPK and KLHL20. In cells treated with IFN, a large fraction of KLHL20 is recruited to PML-NBs, thus decreasing the availability of KLHL20 to its substrate DAPK (Figure 8D, right panel). IFN signalling is known to transactivate PML promoter (Lavau *et al*, 1995; Stadler *et al*, 1995), thereby increasing PML protein level and PML-NBs. We found that DAPK and PML compete for binding KLHL20, which likely accounts for the enrichment of KLHL20 in PML-NBs and disruption of KLHL20–DAPK complex in IFN-treated cells. In support of this notion, PML depletion abolishes IFN-induced relocation of KLHL20 and reverses the inhibitory effect of IFN on KLHL20-mediated DAPK ubiquitination and degradation. Thus, our study reveals that IFN induces DAPK stabilization by suppressing KLHL20-mediated DAPK polyubiquitination. Although DAPK is not a short-lived protein (endogenous DAPK with a half-life ∼7 h in MEF), inhibition of DAPK ubiquitination by IFN did significantly increase DAPK half-life and steady-state protein level. Of note, DAPK has long been known to be a mediator of IFN-induced cell death (Deiss *et al*, 1995). Although one earlier study found that IFN-γ induces the transcriptional activation of DAPK *via* C/EBP-β (Gade *et al*, 2008), we identify a posttranslational mechanism by which IFN triggers DAPK stabilization. Intriguingly, although IFN upregulates the expression of DAPK, it does not significantly elevate the level of S308-phosphorylated DAPK (Supplementary Figure S11), which represents an auto-inactivated form of DAPK (Shohat *et al*, 2001). This finding suggests that IFN also promotes DAPK activation, presumably through the action of a phosphatase. We believe that all three mechanisms, that is, transcriptional activation, stabilization, and relieving the autoinhibition, may act in concert to achieve the maximal induction of DAPK activity in IFN-treated cells. The existence of multiple pathways for DAPK upregulation by IFN highlights the importance of this proapoptotic and proautophagic protein in IFN-induced cell death.

We present evidence showing that the blockage of KLHL20-mediated DAPK degradation contributes at least in part to IFN-induced apoptotic and autophagic death. IFN-α has been commonly used as a therapeutic agent in the treatment of certain types of human malignancies, including MM (Gutterman, 1994; Fritz and Ludwig, 2000; Ludwig and Fritz, 2000). However, the effectiveness of IFN-α-based therapy varies among patients. Using both IFN-sensitive and IFN-resistant MMs, we show that the capability of blocking KLHL20-mediated DAPK degradation by sequestration of KLHL20 in PML-NBs has a determining function in MM responsiveness to IFN. The same mechanism may also control the IFN-α responsiveness of hepatocellular carcinoma, as the importance of PML induction in IFN-α-induced apoptosis has been shown in this type of cancer (Herzer *et al*, 2009). Of note, although both PML (Wang *et al*, 1998) and DAPK (Deiss *et al*, 1995) are known to be involved in IFN-induced cell death, our findings assign DAPK as a downstream effector of PML in this death pathway. PML and PML-NBs seem to broadly regulate cell death decisions through different, pathway-specific molecular mechanisms (Krieghoff-Henning and Hofmann, 2008). Identification of a crucial function of PML-dependent DAPK stabilization in IFN-induced apoptosis not only provides new insights into the functional role of PML in this death paradigm, but also facilitates a better understanding of IFN resistance in certain types of tumors.

We show that the DD of DAPK is important for binding KLHL20. However, the DD deletion mutant (DAPKΔDD) displays a residual KLHL20-binding activity, indicating the existence of additional and yet low-affinity binding motif. The presence of more than one adaptor binding sites is analogous to substrates of two other BTB family proteins, Keap1 (Lo *et al*, 2006; Tong *et al*, 2006; Padmanabhan *et al*, 2006, 2008) and SPOP (Zhuang *et al*, 2009). Furthermore, a recent structural study reported that the ability of SPOP to engage multiple-binding sites in one substrate is attributed to

its structural flexibility and dimerization ability (Zhuang *et al*, 2009). Perhaps KLHL20 adapts a similar mechanism for substrate binding. Nevertheless, the DD of DAPK should contain the primary site for KLHL20 binding, as DAPKΔDD is almost completely refractory to KLHL20-mediated ubiquitination. We believe that this resistance to KLHL20 explains why the overexpression of DAPKΔDD reverses the antiapoptotic effect of KLHL20, even though our earlier study indicates that DAPKΔDD elicits a weaker proapoptotic activity than the wild-type protein (Chen *et al*, 2005).

Unlike many substrates for Cul1-based ligases (Petroski and Deshaies, 2005), there is no evidence that posttranslational modifications on substrates are required for their interactions with Cul3-based ligases. Furthermore, in the cases of two BTB family proteins, Keap1 (Lo *et al*, 2006) and SPOP (Zhuang *et al*, 2009), substrate phosphorylation inhibits rather than promotes their recruitment. It is unknown whether DAPK posttranslational modifications could regulate its turnover by KLHL20. Of note, studies on Keap1 have revealed a different mode for regulating Cul3-based ubiquitination. Under oxidative or electrophilic stress, modifications of several redox-sensitive cysteine residues on Keap1 inhibit the ubiquitination activity of Cul3–Keap1 complex (Zhang and Hannink, 2003; Wakabayashi *et al*, 2004). Interestingly, comparing the regulatory mechanisms between KLHL20-mediated DAPK ubiquitination and Keap1-mediated Nrf2 ubiquitination reveals several similarities. First, in both cases, substrates are constitutively targeted to the Cul3-based ligase complexes under basal conditions. Second, extracellular or intracellular signal capable of regulating the two Cul3-dependent ubiquitination events induces an off signal on the ubiquitination. Third, in both cases, regulation of substrate ubiquitination occurs at the level of substrate adaptor, rather than substrate itself. Notably, all these features are in sharp contrast with the general regulatory principle of Cul1-dependent ubiquitination, in which substrate modification induced by a stimulus often switches on the ubiquitination event.

Earlier reports revealed that DAPK ubiquitination/degradation can also be mediated by a HECT family E3 ligase mind-bomb1 (Mib1) (Zhang *et al*, 2007) and a U-box-containing E3 ligase CHIP (Zhang *et al*, 2007). Our identification of ROC1–Cul3–KLHL20 as a *bona fide* DAPK E3 ligase further expands the repertoire of DAPK E3 ligases and highlights the importance of ubiquitination/proteasomal degradation process in regulating DAPK. Consistent with this notion, it has been shown that DAPK protein expression is uncoupled from its mRNA expression under certain stress conditions (Lin *et al*, 2007). Importantly, although inhibition of both Mib1- and CHIP-mediated DAPK ubiquitination is implicated in DAPK stabilization induced by HSP90 (Zhang *et al*, 2007), suppression of KLHL20-mediated DAPK degradation is responsible for DAPK induction by IFN. Thus, different extracellular and intracellular signals could act on distinct E3 ligases to regulate DAPK protein level. It would be interesting to determine whether modulation of DAPK ubiquitination/degradation occurs in other death systems.

Materials and methods

Cell culture, transient transfection, and retroviral infection

293T, HeLa, NIH3T3, wild-type and PML$^{-/-}$ MEF cells (provided by Gerd Maul) were cultured in Dulbecco's modified Eagle's medium (DMEM) supplemented with 10% fetal calf serum (FCS). H929 cells (provided by Kuo-I Lin) were maintained in RPMI 1640 medium supplemented with 10% FCS and 50 μM 2-mercaptoethanol (2-ME). XG1 cells (provided by Qing Yi) were cultured in RPMI 1640 medium supplemented with 10% FCS, 50 μM 2-ME, 2 mM L-glutamine, and 10 ng/ml human interleukin-6 (R&D Systems). MCF7 cells were cultured in DMEM/F12 medium supplemented with 10% FCS, nonessential amino acid, and 20 mM L-glutamine. Transfections were performed using the calcium phosphate method or the Lipofectamine 2000 reagent. Retroviral infection was performed as described earlier (Kuo *et al*, 2006).

Plasmids

The expression constructs for wild type and various mutants of DAPK with C-terminal Myc or Flag tag were described (Jang *et al*, 2002; Kuo *et al*, 2003; Chen *et al*, 2005). The KLHL20 cDNA (FLJ10568/AK001430) was purchased from Helix Research Institute, Japan, and then subcloned to pRK5-Flag, pRK5-Myc, or pLenti6/V5-GW/lacZ vector. The Kelch-repeat domain deletion mutant (KLHL20ΔK: residues 1–316) and the BTB domain deletion mutant (KLHL20ΔB: residues 301–609) were generated by PCR. The KLHL20m6 mutant, in which the residues 109, 111, 113, 146, 148, and 150 were each replaced by an alanine residue, was generated by site-directed mutagenesis. pMyc-ubiquitin was a gift from Zee-Fen Chang. pCDNA3-Myc-hCul3 and 3xMyc-ROC1 were provided by Yue Xiong. pCDNA3-Myc-hCul3$^{\Delta ROC1}$ (deletion of residues 597–615) was generated by site-directed mutagenesis. pEBB-Cul3-NTD was provided by Christopher Carpenter.

Antibodies and reagents

Polyclonal antibody to DAPK was described earlier (Jang *et al*, 2002). Anti-Myc (9E10) and anti-human PML (H-238: for western blot; PGM3: for immunostaining) antibodies were obtained from Santa Cruz. Anti-Flag (M2) antibody, pS308-DAPK antibody, human IFN-α, and cycloheximide were purchased from Sigma. Human and mouse IFN-γ were from R&D Systems. Anti-mouse PML and anti-α-tubulin antibodies were obtained from Upstate, whereas anti-Cul3 antibody and anti-LC3 antibody were from Cell Signaling. MG132 was purchased from CALBIOCHEM. To generate antiserum against KLHL20, a KLHL20 N-terminal segment (residues 1–139) was cloned to pET30a vector to generate 6xHis-tagged fusion protein. The fusion protein was purified using the Ni-chelating HisTrap affinity column (Amersham) under denaturing condition. The purified protein was used to immunize rabbits and the resulting antiserum was affinity purified.

Immunoprecipitation

Immunoprecipitation using cell lysates containing equal amounts of proteins was performed as described earlier (Chen *et al*, 2005).

Yeast two-hybrid screen

Yeast two-hybrid screen of a human placenta cDNA library using the DD of DAPK as bait was described earlier (Chen *et al*, 2005). To verify the interaction between DAPK DD and KLHL20 by one-on-one transformation assays, yeast strain L40 was cotransformed with pACT2-Gal4-AH3 (encoding amino acid 174–609 of KLHL20 fused with Gal4 activation domain) and pBTM116-LexA-DD (encoding DD of DAPK fused with LexA DNA-binding domain) or pBTM116-LexA-Lamin (as a negative control).

In vitro ubiquitination assay

ROC1–Cul3–KLHL20 complex was purified using Glutathione-Sepharose beads from lysates of 293T cells transfected with GST-Cul3, Myc-KLHL20, and Myc-ROC1. The purified complex bound on beads was incubated at 37°C for 4 h in a 20 μl reaction mixture containing 50 mM Tris–HCl (pH 7.5), 5 mM $MgCl_2$, 1 μM ubiquitin aldehyde, 20 μM MG132, 2 mM ATP, 2 mM NaF, 1 mM DTT, 10 μg ubiquitin, 10 mM creatine phosphate, 0.5 μg creatine kinase, 40 ng yeast E1, 200 ng E2 (UbcH5a), and 300 ng Flag-tagged DAPK purified from baculovirus. All ubiquitin-related reagents were purchased from Boston Biochemicals.

Immunofluorescence analysis

To detect the subcellular localization of KLHL20, cells were fixed and permeabilized with ice-cold methanol for 10 min, and then blocked with PBS supplemented with 10% goat serum, and 1% BSA for 1 h. Next, cells were incubated with various primary antibodies

diluted in PBS containing 0.2% BSA and 5% goat serum for 2 h, and then with FITC- or rhodamine-conjugated anti-mouse or anti-rabbit secondary antibody together with 1 μg/ml of DAPI for 1 h. Cells were then washed, mounted, and examined by a Zeiss LSM510 confocal microscope, using × 100 oil objective lens. To detect the GFP-LC3 signal, cells were fixed with 4% formaldehyde for 20 min and examined by a Zeiss LSM510 confocal microscope equipped with a × 100 oil objective lens or by an epifluorescent microscope (Olympus BX50) equipped with a × 60 oil objective lens. Fluorescent images were captured with a cooled CCD camera operated by a Laser Scanning Microscope LSM510 Software or with an Olympus DP71 digital camera operated by a DP controller.

Production of baculovirus

Monolayers of Sf-21 cells cultured in Grace's medium (Life Technologies) supplemented with 10% FCS were cotransfected with linearized virus DNA (BaculoGold, BD Pharmingen) and pVL1392-based vector. The recombinant virus was harvested, amplified, and then used to infect monolayers of Sf-21 cells in TNM-FH medium (Applichem). After a 3-day incubation, the Flag-tagged recombinant protein was purified using the anti-Flag M2 agarose (Sigma), and then eluted with the Flag peptide.

Apoptosis assay

DAPK-induced apoptosis was assayed as described earlier (Wang *et al*, 2002). To assay IFN-α-induced apoptosis, cells were treated with IFN-α at 2000 U/ml for 48 h. Annexin V staining was performed using the Annexin V-APC kit (BD Pharmingen).

Lentivirus production

Lentivirus carrying DAPK-, KLHL20-, or PML-specific siRNA was used to knockdown DAPK, KLHL20, or PML, respectively. The target sequences of various siRNAs are DAPK siRNA #1: 5′-CAAGA AACGTTAGCAAATG-3′, DAPK siRNA #2: 5′-GGTCAAGGATCCAAA GAAG-3′, KLHL20 siRNA #1: 5′-GGTGGCGTAGGAGTTATTAA-3′, KLHL20 siRNA #2: 5′-GCCTGCTGTGAATTCTTAA-3′, PML siRNA #1: 5′-CACCCGCAAGACCAACAACAT-3′, and PML siRNA #2: 5′-GTG TACCGGCAGATTGTGGAT-3′. To generate recombinant lentivirus, 293FT cells were cotransfected with the package, envelop and siRNA (or cDNA)-expressing constructs. The supernatant containing the virus was harvested, concentrated by ultracentrifugation, and then used to infect cells. For infection of XG1 or H929 cells, the viral stock was supplemented with 8 μg/ml of polybrene, and the infected cells were selected by 2 μg/ml of puromycin, 10 μg/ml of blasticidin, or 125 μg/ml of hygromycin.

Autophagy assay

MCF7 cells were transfected with GFP-LC3 and stable transfectants (MCF-LC3 cells) were isolated by a fluorescent cell sorter. To assay autophagic activity, parental MCF7 cells or MCF7-LC3 cells were transfected with various cDNAs and/or DAPK siRNA together with mCherry-expressing construct. One day after transfection, cells were treated with IFN-γ at 2000 U/ml for 48 h and then analysed by epifluorescent or confocal microscopy for the appearance of GFP-LC3 dots or by western blot for the conversion of LC3-I to LC3-II. In some experiments, cells were treated with 10 μg/ml of E64d and 10 μg/ml of pepstatin A for 16 h to block the lysosomal degradation pathway. To quantify LC3 dots, 50 mCherry-positive cells of each population were randomly chosen for counting the number of LC3 dots per cell.

Supplementary data

Supplementary data are available at *The EMBO Journal* Online (http://www.embojournal.org).

Acknowledgements

We thank Yue Xiong (University of North Carolina at Chapel Hill), Zee-Fen Chang (National Taiwan University), Christopher Carpenter (Harvard Medical School), Kuo-I Lin (Academia Sinica), Qing Yi (The University of Texas MD Anderson Cancer Center), Gerd Maul (The Wistar Institute), and National RNAi Core Facility for providing various constructs or cell lines, Chin-Chun Hung for confocal analyses, and James Steed for editing the manuscript. This work was supported by NSC Frontier Grant NSC98-2321-B-001-037 and Academia Sinica Investigator Award.

Conflict of interest

The authors declare that they have no conflict of interest.

References

Bialik S, Bresnick AR, Kimchi A (2004) DAP-kinase-mediated morphological changes are localization dependent and involve myosin-II phosphorylation. *Cell Death Differ* **11:** 631–644

Bialik S, Kimchi A (2004) DAP-kinase as a target for drug design in cancer and diseases associated with accelerated cell death. *Semin Cancer Biol* **14:** 283–294

Bosu DR, Kipreos ET (2008) Cullin-RING ubiquitin ligases: global regulation and activation cycles. *Cell Div* **3:** 7

Cardozo T, Pagano M (2004) The SCF ubiquitin ligase: insights into a molecular machine. *Nat Rev Mol Cell Biol* **5:** 739–751

Castets M, Coissieux MM, Delloye-Bourgeois C, Bernard L, Delcros JG, Bernet A, Laudet V, Mehlen P (2009) Inhibition of endothelial cell apoptosis by netrin-1 during angiogenesis. *Dev Cell* **16:** 614–620

Chen CH, Wang WJ, Kuo JC, Tsai HC, Lin JR, Chang ZF, Chen RH (2005) Bidirectional signals transduced by DAPK-ERK interaction promote the apoptotic effect of DAPK. *EMBO J* **24:** 294–304

Cohen O, Inbal B, Kissil JL, Raveh T, Berissi H, Spivak-Kroizaman T, Feinstein E, Kimchi A (1999) DAP-kinase participates in TNF-alpha- and Fas-induced apoptosis and its function requires the death domain. *J Cell Biol* **146:** 141–148

Crowder C, Dahle O, Davis RE, Gabrielsen OS, Rudikoff S (2005) PML mediates IFN-alpha-induced apoptosis in myeloma by regulating TRAIL induction. *Blood* **105:** 1280–1287

Cullinan SB, Gordan JD, Jin J, Harper JW, Diehl JA (2004) The Keap1-BTB protein is an adaptor that bridges Nrf2 to a Cul3-based E3 ligase: oxidative stress sensing by a Cul3-Keap1 ligase. *Mol Cell Biol* **24:** 8477–8486

Deiss LP, Feinstein E, Berissi H, Cohen O, Kimchi A (1995) Identification of a novel serine/threonine kinase and a novel 15-kD protein as potential mediators of the gamma interferon-induced cell death. *Genes Dev* **9:** 15–30

Deshaies RJ (1999) SCF and Cullin/Ring H2-based ubiquitin ligases. *Annu Rev Cell Dev Biol* **15:** 435–467

Eisenberg-Lerner A, Kimchi A (2007) DAP kinase regulates JNK signaling by binding and activating protein kinase D under oxidative stress. *Cell Death Differ* **14:** 1908–1915

Fritz E, Ludwig H (2000) Interferon-alpha treatment in multiple myeloma: meta-analysis of 30 randomised trials among 3948 patients. *Ann Oncol* **11:** 1427–1436

Furukawa M, He YJ, Borchers C, Xiong Y (2003) Targeting of protein ubiquitination by BTB-Cullin 3-Roc1 ubiquitin ligases. *Nat Cell Biol* **5:** 1001–1007

Furukawa M, Xiong Y (2005) BTB protein Keap1 targets antioxidant transcription factor Nrf2 for ubiquitination by the Cullin 3-Roc1 ligase. *Mol Cell Biol* **25:** 162–171

Gade P, Roy SK, Li H, Nallar SC, Kalvakolanu DV (2008) Critical role for transcription factor C/EBP-beta in regulating the expression of death-associated protein kinase 1. *Mol Cell Biol* **28:** 2528–2548

Geyer R, Wee S, Anderson S, Yates J, Wolf DA (2003) BTB/POZ domain proteins are putative substrate adaptors for cullin 3 ubiquitin ligases. *Mol Cell* **12:** 783–790

Gozuacik D, Bialik S, Raveh T, Mitou G, Shohat G, Sabanay H, Mizushima N, Yoshimori T, Kimchi A (2008) DAP-kinase is a mediator of endoplasmic reticulum stress-induced caspase activation and autophagic cell death. *Cell Death Differ* **15:** 1875–1886

Gutterman JU (1994) Cytokine therapeutics: lessons from interferon alpha. *Proc Natl Acad Sci USA* **91:** 1198–1205

Hara T, Ishida H, Raziuddin R, Dorkhom S, Kamijo K, Miki T (2004) Novel kelch-like protein, KLEIP, is involved in actin assembly at cell-cell contact sites of Madin-Darby canine kidney cells. *Mol Biol Cell* **15:** 1172–1184

Harrison B, Kraus M, Burch L, Stevens C, Craig A, Gordon-Weeks P, Hupp TR (2008) DAPK-1 binding to a linear peptide motif in MAP1B stimulates autophagy and membrane blebbing. *J Biol Chem* **283:** 9999–10014

Hershko A, Ciechanover A (1998) The ubiquitin system. *Annu Rev Biochem* **67:** 425–479

Herzer K, Hofmann TG, Teufel A, Schimanski CC, Moehler M, Kanzler S, Schulze-Bergkamen H, Galle PR (2009) IFN-{alpha}-induced apoptosis in hepatocellular carcinoma involves promyelocytic leukemia protein and TRAIL independently of p53. *Cancer Res* **69:** 855–862

Inbal B, Bialik S, Sabanay I, Shani G, Kimchi A (2002) DAP kinase and DRP-1 mediate membrane blebbing and the formation of autophagic vesicles during programmed cell death. *J Cell Biol* **157:** 455–468

Inbal B, Cohen O, Polak-Charcon S, Kopolovic J, Vadai E, Eisenbach L, Kimchi A (1997) DAP kinase links the control of apoptosis to metastasis. *Nature* **390:** 180–184

Jackson PK, Eldridge AG (2002) The SCF ubiquitin ligase: an extended look. *Mol Cell* **9:** 923–925

Jang CW, Chen CH, Chen CC, Chen JY, Su YH, Chen RH (2002) TGF-beta induces apoptosis through Smad-mediated expression of DAP- kinase. *Nat Cell Biol* **4:** 51–58

Kobayashi A, Kang MI, Okawa H, Ohtsuji M, Zenke Y, Chiba T, Igarashi K, Yamamoto M (2004) Oxidative stress sensor Keap1 functions as an adaptor for Cul3-based E3 ligase to regulate proteasomal degradation of Nrf2. *Mol Cell Biol* **24:** 7130–7139

Krek W (2003) BTB proteins as henchmen of Cul3-based ubiquitin ligases. *Nat Cell Biol* **5:** 950–951

Krieghoff-Henning E, Hofmann TG (2008) Role of nuclear bodies in apoptosis signalling. *Biochim Biophys Acta* **1783:** 2185–2194

Kuo J-C, Lin J-R, Staddon JM, Hosoya H, Chen R-H (2003) Uncoordinated regulation of stress fibers and focal adhesions by DAP-kinase. *J Cell Sci* **116:** 4777–4790

Kuo JC, Wang WJ, Yao CC, Wu PR, Chen RH (2006) The tumor suppressor DAPK inhibits cell motility by blocking the integrin-mediated polarity pathway. *J Cell Biol* **172:** 619–631

Lavau C, Marchio A, Fagioli M, Jansen J, Falini B, Lebon P, Grosveld F, Pandolfi PP, Pelicci PG, Dejean A (1995) The acute promyelocytic leukaemia-associated PML gene is induced by interferon. *Oncogene* **11:** 871–876

Lin Y, Stevens C, Hupp T (2007) Identification of a dominant negative functional domain on DAPK-1 that degrades DAPK-1 protein and stimulates TNFR-1-mediated apoptosis. *J Biol Chem* **282:** 16792–16802

Llambi F, Lourenco FC, Gozuacik D, Guix C, Pays L, Del Rio G, Kimchi A, Mehlen P (2005) The dependence receptor UNC5H2 mediates apoptosis through DAP-kinase. *EMBO J* **24:** 1192–1201

Lo SC, Li X, Henzl MT, Beamer LJ, Hannink M (2006) Structure of the Keap1: Nrf2 interface provides mechanistic insight into Nrf2 signaling. *EMBO J* **25:** 3605–3617

Ludwig H, Fritz E (2000) Interferon in multiple myeloma—summary of treatment results and clinical implications. *Acta Oncol* **39:** 815–821

Padmanabhan B, Tong KI, Kobayashi A, Yamamoto M, Yokoyama S (2008) Structural insights into the similar modes of Nrf2 transcription factor recognition by the cytoplasmic repressor Keap1. *J Synchrotron Radiat* **15:** 273–276

Padmanabhan B, Tong KI, Ohta T, Nakamura Y, Scharlock M, Ohtsuji M, Kang MI, Kobayashi A, Yokoyama S, Yamamoto M (2006) Structural basis for defects of Keap1 activity provoked by its point mutations in lung cancer. *Mol Cell* **21:** 689–700

Pelled D, Raveh T, Riebeling C, Fridkin M, Berissi H, Futerman AH, Kimchi A (2002) Death-associated protein (DAP) kinase plays a central role in ceramide-induced apoptosis in cultured hippocampal neurons. *J Biol Chem* **277:** 1957–1961

Petroski MD, Deshaies RJ (2005) Function and regulation of cullin-RING ubiquitin ligases. *Nat Rev Mol Cell Biol* **6:** 9–20

Pintard L, Willems A, Peter M (2004) Cullin-based ubiquitin ligases: Cul3-BTB complexes join the family. *EMBO J* **23:** 1681–1687

Pintard L, Willis JH, Willems A, Johnson JL, Srayko M, Kurz T, Glaser S, Mains PE, Tyers M, Bowerman B, Peter M (2003) The BTB protein MEL-26 is a substrate-specific adaptor of the CUL-3 ubiquitin-ligase. *Nature* **425:** 311–316

Raval A, Tanner SM, Byrd JC, Angerman EB, Perko JD, Chen SS, Hackanson B, Grever MR, Lucas DM, Matkovic JJ, Lin TS, Kipps TJ, Murray F, Weisenburger D, Sanger W, Lynch J, Watson P, Jansen M, Yoshinaga Y, Rosenquist R *et al* (2007) Downregulation of death-associated protein kinase 1 (DAPK1) in chronic lymphocytic leukemia. *Cell* **129:** 879–890

Raveh T, Droguett G, Horwitz MS, DePinho RA, Kimchi A (2001) DAP kinase activates a p19ARF/p53-mediated apoptotic checkpoint to suppress oncogenic transformation. *Nat Cell Biol* **3:** 1–7

Shohat G, Spivak-Kroizman T, Cohen O, Bialik S, Shani G, Berrisi H, Eisenstein M, Kimchi A (2001) The pro-apoptotic function of death-associated protein kinase is controlled by a unique inhibitory autophosphorylation-based mechanism. *J Biol Chem* **276:** 47460–47467

Stadler M, Chelbi-Alix MK, Koken MH, Venturini L, Lee C, Saib A, Quignon F, Pelicano L, Guillemin MC, Schindler C, de The H (1995) Transcriptional induction of the PML growth suppressor gene by interferons is mediated through an ISRE and a GAS element. *Oncogene* **11:** 2565–2573

Stogios PJ, Downs GS, Jauhal JJ, Nandra SK, Prive GG (2005) Sequence and structural analysis of BTB domain proteins. *Genome Biol* **6:** R82

Strander H, Einhorn S (1996) Interferons and the tumor cell. *Biotherapy* **8:** 213–218

Tong KI, Katoh Y, Kusunoki H, Itoh K, Tanaka T, Yamamoto M (2006) Keap1 recruits Neh2 through binding to ETGE and DLG motifs: characterization of the two-site molecular recognition model. *Mol Cell Biol* **26:** 2887–2900

Wakabayashi N, Dinkova-Kostova AT, Holtzclaw WD, Kang MI, Kobayashi A, Yamamoto M, Kensler TW, Talalay P (2004) Protection against electrophile and oxidant stress by induction of the phase 2 response: fate of cysteines of the Keap1 sensor modified by inducers. *Proc Natl Acad Sci USA* **101:** 2040–2045

Wang WJ, Kuo JC, Ku W, Lee YR, Lin FC, Chang YL, Lin YM, Chen CH, Huang YP, Chiang MJ, Yeh SW, Wu PR, Shen CH, Wu CT, Chen RH (2007) The tumor suppressor DAPK is reciprocally regulated by tyrosine kinase Src and phosphatase LAR. *Mol Cell* **27:** 701–716

Wang WJ, Kuo JC, Yao CC, Chen RH (2002) DAP-kinase induces apoptosis by suppressing integrin activity and disrupting matrix survival signals. *J Cell Biol* **159:** 169–179

Wang ZG, Ruggero D, Ronchetti S, Zhong S, Gaboli M, Rivi R, Pandolfi PP (1998) PML is essential for multiple apoptotic pathways. *Nat Genet* **20:** 266–272

Willems AR, Schwab M, Tyers M (2004) A hitchhiker's guide to the cullin ubiquitin ligases: SCF and its kin. *Biochim Biophys Acta* **1695:** 133–170

Xu L, Wei Y, Reboul J, Vaglio P, Shin TH, Vidal M, Elledge SJ, Harper JW (2003) BTB proteins are substrate-specific adaptors in an SCF-like modular ubiquitin ligase containing CUL-3. *Nature* **425:** 316–321

Zalckvar E, Berissi H, Mizrachy L, Idelchuk Y, Koren I, Eisenstein M, Sabanay H, Pinkas-Kramarski R, Kimchi A (2009) DAP-kinase-mediated phosphorylation on the BH3 domain of beclin 1 promotes dissociation of beclin 1 from Bcl-XL and induction of autophagy. *EMBO Rep* **10:** 285–292

Zhang DD, Hannink M (2003) Distinct cysteine residues in Keap1 are required for Keap1-dependent ubiquitination of Nrf2 and for stabilization of Nrf2 by chemopreventive agents and oxidative stress. *Mol Cell Biol* **23:** 8137–8151

Zhang DD, Lo SC, Cross JV, Templeton DJ, Hannink M (2004) Keap1 is a redox-regulated substrate adaptor protein for a Cul3-dependent ubiquitin ligase complex. *Mol Cell Biol* **24:** 10941–10953

Zhang L, Nephew KP, Gallagher PJ (2007) Regulation of death-associated protein kinase. Stabilization by HSP90 heterocomplexes. *J Biol Chem* **282:** 11795–11804

Zhuang M, Calabrese MF, Liu J, Waddell MB, Nourse A, Hammel M, Miller DJ, Walden H, Duda DM, Seyedin SN, Hoggard T, Harper JW, White KP, Schulman BA (2009) Structures of SPOP-substrate complexes: insights into molecular architectures of BTB-Cul3 ubiquitin ligases. *Mol Cell* **36:** 39–50